Bioorganic & Medicinal Chemistry 18 (2010) 8341–8349

Contents lists available at ScienceDirect

Bioorganic & Medicinal Chemistry

journal homepage: www.elsevier.com/locate/bmc

Virtual screening against nuclear factor κB (NF-κB) of a focus library: Identification of bioactive furocoumarin derivatives inhibiting NF-κB dependent biological functions involved in cystic fibrosis

Laura Piccagli [a,*], Monica Borgatti [a], Elena Nicolis [b], Nicoletta Bianchi [a], Irene Mancini [a], Ilaria Lampronti [a], Daniela Vevaldi [c], Francesco Dall'Acqua [c], Giulio Cabrini [a], Roberto Gambari [a,*]

[a] BioPharmaNet, Department of Biochemistry and Molecular Biology, Interdisciplinary Center for the Study of Inflammation, Via L. Borsari 46, I-44100 Ferrara, Italy
[b] Laboratory of Molecular Pathology, Laboratory of Clinical Chemistry and Haematology, University-Hospital, Verona, Italy
[c] Department of Pharmaceutical Science, University of Padova, Italy

ARTICLE INFO

Article history:
Received 17 May 2010
Revised 22 September 2010
Accepted 24 September 2010
Available online 1 October 2010

Keywords:
NF-κB
Virtual screening
Inhibitors
Furocoumarin
Cystic fibrosis

ABSTRACT

In the present study, a structured-based virtual screening (VS) of differently substituted furocoumarins and analogues has been carried out against nuclear factor kappa B (NF-κB), with the objective of selecting molecules able to inhibit the binding of this transcription factor to the DNA. The focus library was developed starting from chemical structures obtained from the literature, as well as retrieving compounds from available commercial databases. A two dimensional substructure searching method based on four different chemical scaffolds was used for this purpose. Among the 10 highest-scored ligands selected from the docking studies, five commercially available molecules were investigated in biological assays. Four furocoumarin derivatives showed IC_{50} values in the range of 40–100 μM in inhibiting NF-κB/DNA interactions studied by electrophoretic mobility shift assay (EMSA). Three compounds significantly inhibited NF-κB dependent biological functions (expression of IL-8) in cellular analysis based on *Pseudomonas aeruginosa* infection of cystic fibrosis IB3-1 cells. These findings validated the virtual screening approach here presented and reinforce the successful results of our previously computational studies aimed at the identification of molecules targeting NF-κB. The discovered novel compounds could be of relevance to identify more potent inhibitors of NF-κB dependent biological functions beneficial to control lung inflammation occurring in patients affected by cystic fibrosis.

1. Introduction

Cystic fibrosis (CF) is a genetic disease caused by mutations of the Cystic Fibrosis Transmembrane Conductance Regulator (CFTR) gene, which encodes for a chloride channel.[1,2] Although CFTR is expressed in several epithelia, the consequences of mutated CFTR for morbidity and mortality of CF patients are most important in the respiratory tract.[3] Mutations in CFTR impair the mucociliary clearance, due to reduced periciliary fluid volume and increased viscosity of submucosal gland secretions, leading to chronic bacterial infections, mostly caused *Pseudomonas aeruginosa*.[1–4]

The hallmark of the CF airway pathology is the elevated secretion of several pro-inflammatory cytokines and chemokines, such as for instance IL-1β, IL-6, TNF-α and IL-8, which have been found in the airway fluid of CF patients.[5] With respect to pro-inflammatory mechanisms, *P. aeruginosa* products interact with Toll-like and asialo GM1 receptors expressed on bronchial epithelial cells, leading to (a) downstream activation of nuclear transcription factors, including NF-κB[6–8] and (b) transcription of a cascade of pro-inflammatory cytokines and chemokines, first of all the NF-κB dependent IL-8,[9–11] which is well-known to play a crucial role in PMN recruitment in CF lung.[12] In the presence of bacteria, airway epithelial cells initiate the innate immune response, in which NF-κB-dependent gene transcription is heavily involved.

In a recent paper, we have used natural products as sources for the discovery of new drugs on the basis of their ability to interfere with protein/DNA interactions, including inhibition of NF-κB activity.[13,14] We found that the whole extract of *Aegle marmelos* has the strongest inhibitory effect on *P. aeruginosa*-dependent IL-8 induction in human CF-derived bronchial IB3-1 cells without affecting cell proliferation. By separating the major components contained in *A. marmelos* by gas chromatography and identifying their structure by mass spectrometry, we found that three major components, namely 5,6-dimethoxy-1-indanone, 2-hydroxy-cinnamic acid and 5-methoxy psoralen (5-MOP), reproduce the inhibitory effect observed with the whole extract from *A. marmelos*.[15] Of particular interest was, in our opinion, the furocoumarin 5-MOP.[16,17] Although its use in association with Ultraviolet A irradiation for skin diseases

* Corresponding authors. Tel.: +39 0532 974443; fax: +39 0532 974500 (R.G.); tel.: +39 0532 974760 (L.P.).
E-mail addresses: laura.piccagli@unife.it (L. Piccagli), gam@unife.it (R. Gambari).

0968-0896/$ - see front matter © 2010 Elsevier Ltd. All rights reserved.
doi:10.1016/j.bmc.2010.09.063

was known from a long time, our observation was the first report of 5-MOP directed anti-inflammatory effect in the absence of irradiation. In this respect, interactions of furocoumarins with the transcription nuclear factor NF-κB might take place, as suggested in elsewhere published studies.[15]

In addition to direct screening, we have recently reported the possible use of a structured-based VS procedure to identify possible NF-κB binders.[18,19] In this study, VS against NF-κB p50 using docking simulations was applied by starting from a three-dimensional (3D) database containing more than 4.6 million commercially available structures. This database was filtered by specifying a subset of commercially available compounds sharing a (2*E*,*Z*)-3-(2-hydroxyphenyl)-2-propenoate substructure and relevant drug like properties. Docking simulations to p50 NF-κB were performed with a test set of six known inhibitors of NF-κB/DNA interactions.[18,19] In agreement with docking results, the highest-scored compound (compound **1**, see Fig. 1) displayed a high level of inhibitory activity in electrophoretic mobility shift assay (EMSA) experiments (inhibition of NF-κB/DNA interactions)[20,21] and on biological functions dependent on NF-κB activity (inhibition of IL-8 gene expression in cystic fibrosis IB3-1 cells).[15,22] We demonstrated that this in silico screening approach is suitable for the identification of low-molecular-weight compounds that inhibit NF-κB/DNA interactions and NF-κB-dependent functions[19], confirming a previously published study.[18]

This and similar approaches are relevant in medicinal chemistry, as information deduced from the discovery of new lead compounds and their binding mode could result in further lead optimization resulting in more potent NF-κB inhibitors.[18,19] In this respect, the VS strategy is one of the most promising in the field of the discovery of novel bioactive compounds, as recently reviewed.[23] Interestingly, the most active compound of our study resulted to be a furocoumarin analogue, with a cyclopentane ring instead of furan function.[19] Therefore, in the present study we constructed a focus library of differently substituted furocoumarins and analogues for an in silico screening against NF-κB, with the aim of finding more potent NF-κB inhibitors.

2. Results and discussion

The outline of the experimental strategy was the following: first, the construction of a large furocoumarin-like data base; second, the virtual screening of this database against NF-κB by means of docking procedures; third, the study of the poses on NF-κB of the most interesting selected compounds. After these bioinformatic analyses, we validated the results obtained using two complementary biological systems, electrophoretic mobility shift assay (EMSA),[24,25] to study the effects of the selected compounds on NF-κB/DNA interactions and treatment of cystic fibrosis IB3-1

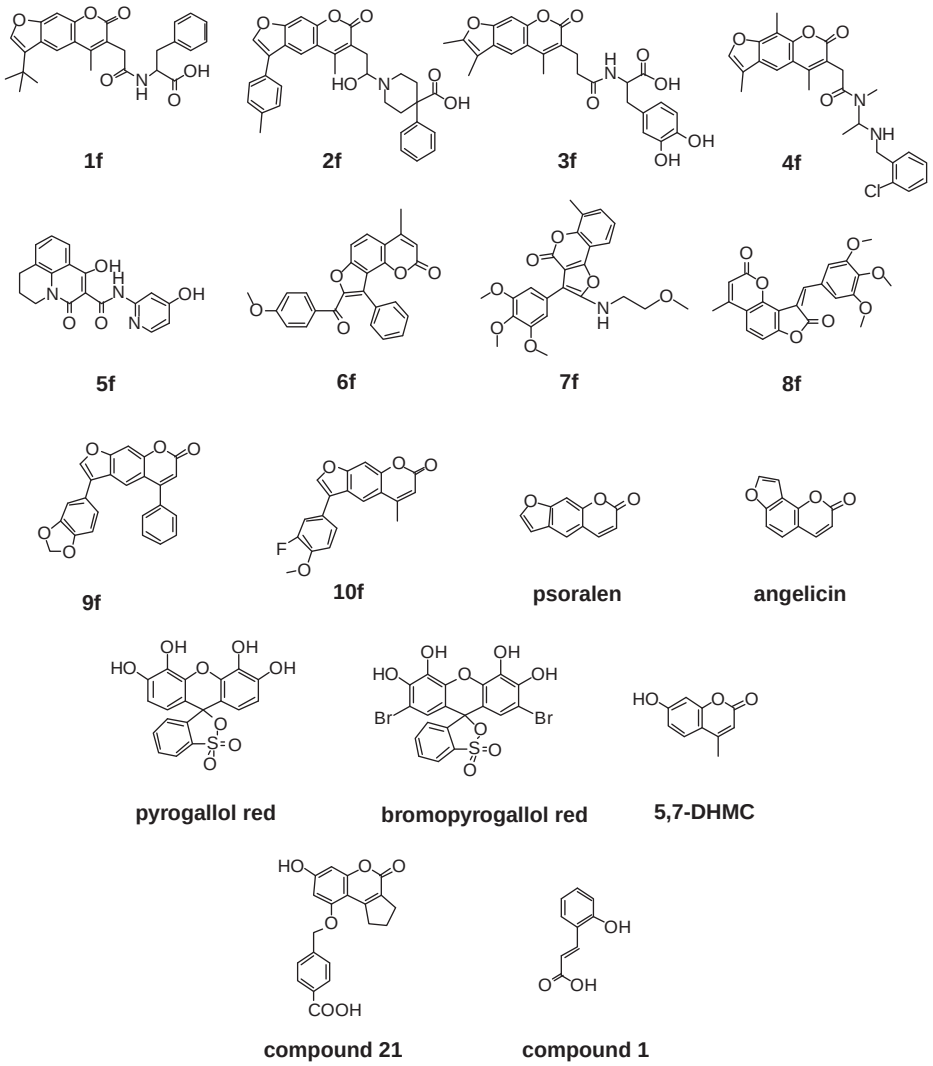

Figure 1. Chemical two dimensional structures of hits from VS against NF-κB and other known NF-κB inhibitors.

cells infected by *P. aeruginosa*,[21] to study the effects on the expression of the NF-κB regulated IL-8 gene.

2.1. Set up of the focus chemical library

The first step of the present study was the construction of a customized furocoumarin-based small molecules database. The scaffolds for each of the four different classes of the furocoumarin derivatives and analogues, including compounds retrieved from the literature,[26,27] are shown in Table 1. The developed library of 1710 compounds (see experimental section) contained 54 structures of angelicin derivatives (molecular weight range: 186–478), 1384 of psolaren derivatives (molecular weight range: 186–619), 51 of Furo(3,2-c)chromen-4-one structures (molecular weight range: 268–439) and 166 of benzoquinolizin-5-one analogues (molecular weight range: 258–499).

2.2. Molecular docking runs to NF-κB targets

Molecular docking approach was followed against NF-κB in both p50 aggregation states using Glide software in the same procedure previously validated by us[18,19] for this protein target. In Table 2 the docking results of the in silico screening are shown relatively to the first 10 ranked ligands (structures shown in Fig. 1) for the dimer, and the monomer in different conformations. In Figure 1 we also included the chemical structures of references furocoumarins (psoralen and angelicin) as well as references NF-κB inhibitors, such as pyrogallol red,[28] bromopyrogallol red,[28] 5,7-DHMC[29] and, of relevance since they have been selected with a VS procedure similar to that here employed, compounds **1** and **21**, published by Piccagli et al.,[18,19] respectively. These compounds were employed as references for the EMSA studies.

The docking studies were carried out by using the extra precision (XP) method on a subset of 1000 molecules selected by the Standard Precision (SP) procedure performed using the Glide software. The selection of docked compounds was based on the docking GlideScore (G-Score) values in each target. Indeed, G-Score SP is a 'soft' function useful to identify ligands that have a reasonable propensity to form a stable complex with the corresponding molecular target. Glide score XP, on the contrary, is an advanced function that penalizes the poses that violate established physical chemistry principles, such as charged and strongly polar groups that (a) make an appropriate complement of hydrogen bonds or (b) are suitably exposed to solvent. Thus, the SP Glide procedure was here used to reduce the number of molecules to be studied in the more accurate XP docking runs. The docked compounds

Table 1
Chemical scaffold of customized compounds library

Compounds[a]	R1	R2	R3	R4	R5	R6	X	Y
Angelicin scaffold and derivatives								
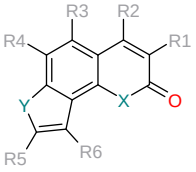								
Angelicin	H	H	H	H	H	H	O	O
4-Methylangelicin	H	CH_3	H	H	H	H	O	O
4,5′-Dimethylangelicin	H	CH_3	H	H	CH_3	H	O	O
6,5-Dimethylangelicin	H	H	CH_3	CH_3	H	H	O	O
4′,5′-Dimethylangelicin	H	H	H	H	CH_3	CH_3	O	O
4,5′,4′-Trimethylangelicin (TMA)	H	CH_3	H	H	CH_3	CH_3	O	O
4,6,2′-Trimethylfluoroquinolinone	H	CH_3	H	CH_3	CH_3	H	NCH_3	O
4,2′,3′-Trimethyltioangelicin	H	CH_3	H	H	CH_3	CH_3	O	S
Psolaren scaffold and derivatives								
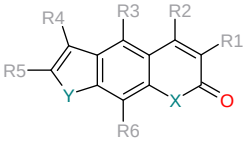								
Psolaren	H	H	H	H	H	H	O	O
4-Methylpsolaren	H	CH_3	H	H	H	H	O	O
5-Methylpsolaren	H	H	CH_3	H	H	H	O	O
4,5′-Dimethylpsolaren	H	CH_3	H	CH_3	H	H	O	O
5,4′-Dimethylpsolaren	H	H	CH_3	CH_3	H	H	O	O
3,4-Dimethylpsolaren	CH_3	CH_3	H	H	H	H	O	O
4,5′,8-Trimethylpsolaren (TMP)	H	CH_3	H	H	CH_3	CH_3	O	O
5-Methoxypsolaren	H	H	OCH_3	H	H	H	O	O
8-Methoxypsolaren	H	H	H	H	H	OCH_3	O	O
5,8 -Methoxypsolaren	H	H	OCH_3	H	H	OCH_3	O	O
4,4′,5′-Trimethylpsolaren	H	CH_3	H	CH_3	CH_3	H	O	S

Furo(3,2-c)chromen-4one Scaffold	Benzoquinolizin-5-one scaffold[b]
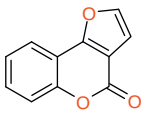	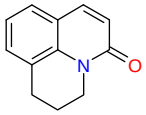

[a] Molecules listed by Viola et al.[24]
[b] Proposed by Miolo et al.[25]

Table 2
Best score of the docked molecules (**1f–10f**) into both NF-κB p50 dimer (p50-p50) and monomers (p50a, p50b, p50*b*)

Compound	GlideScore[a]			
	p50-p50	p50a	p50b	p50*b*
1f	−10.30	/	−6.13	−6.42
2f	−9.65	−6.82	−6.87	/
3f	/	−8.06	−3.14	/
4f	−8.05	−7.01	−6.30	/
5f	/	−7.71	−5.49	/
6f	−7.48	/	/	−6.19
7f	−7.44	/	−6.94	/
8f	−7.30	/	−5.42	/
9f	−7.21	/	/	/
10f	−6.95	/	/	/

[a] Glide Score (G-score) values obtained applying the XP docking method.

showing the best XP G-score values (Table 2) against both separately considered NF-κB targets (monomer and dimer), were selected among the four classes of chemical structures. Moreover, the molecules with higher rank in more than one conformation of the monomer were preferred. This strategy was followed on the basis of our previously published VS study[19] on a data set of known protein binders, in which an increase of the enrichment factor in assembled configurations of p50 has been obtained with more efficiency in respect to the docking application performed on just one conformation of the target macromolecule. Among possible docking hits, two molecules (**9f** and **10f**) were chosen on the basis of their ability to selectively interact to the dimer (monomer G-scores >0).

After this analysis, compound **1f** (the psolaren-like structure best-ranked into the NF-κB dimer, with a G-Score = −10.30 kcal mol^{-1}), the benzoquinolizin-5-one analogue **5f** and the commercially available angelicin derivatives **6f** and **8f**, the furo(3,2-c)chromen-4one derivative **7f**, and the psoralen derivatives **9f** and **10f** were investigated in deep. Finally, the choice of the best-docked structure belonging to the most populated cluster of poses was based on the highest XP G-score and E-model values (combination of energy grid sore, G-score and the internal strain of the ligand) and by visual inspection. Considering the structural feature of NF-κB, as previously discussed by us[19], those molecules placed in proximity of the 10 residues linker (see Fig. 2) should present a similar score and ranking in both monomeric and dimeric state of the protein, as previously reported.[19] On the contrary, ligands localized in or near the region between the N-terminal domains of both p50, are expected to exhibit different G-score depending on the aggregation form of NF-κB. In particular, an increasing of binding affinity should be displayed into the dimer in case of additional stabilizing interactions between the ligand and the other subunit environment.

2.3. Ligand binding modes into NF-κB

All the individuated best ranked ligand poses in both dimer and monomer were localized in the DNA binding surface of the N-terminal domains involved in the formation of the solvent-filled cavity, as in case of active cellular dimeric aggregation process. Relatively to the dimer, as Figures 2 and 3 point out, the selected poses of the best ranked compound **1f** (GlideScore = −10.30 kcal mol^{-1}; E-Model = −52.8 kcal mol^{-1}) and molecules **6f** (GlideScore = −7.43 kcal mol^{-1}; E-Model = −41.8 kcal mol^{-1}), **7f** (GlideScore = −7.27 kcal mol^{-1}; E-Model = −45.5 kcal mol^{-1}), **9f** (GlideScore = −7.21 kcal mol^{-1}; E-Model = −35.7 kcal mol^{-1}) and **10f** (GlideScore = −6.95 kcal mol^{-1}; E-Model = −29.3 kcal mol^{-1}) correspond to a region involved in the binding of compounds **21** and **1**, previously described by us.[19] This area is constituted by residues of both p50 units (chain A and chain B) of NF-κB. All the residues of the protein involved in molecular interactions with the active ligands formed hydrogen bonds also with DNA.

In Table 3 the molecular interactions of **1f, 6f, 7f, 9f** and **10f** with the residues of the DNA binding site of the protein are shown (Figs. 2 and 3). All these different compounds interact preferentially with residues of p50 (chain B) and present a binding mode very similar to compounds **21** and **1**.[18,19] In particular, the amide oxigen of **1f** engages a hydrogen bond with the OH group of Thr143 and its carboxylate group forms a salt bridge stabilized by one hydrogen bond with NH_3^+ function of Lys 145. Moreover, the phenyl structure of compound **1f** is involved in a π–π stacking interaction with the aromatic moiety of Tyr57 which is a residue specific for molecular interactions with the κB DNA sequence 5′-GGGATTTCC-3′, present in different NF-κB regulated cellular genes, and in the HIV-LTR. Moreover, molecule **1f** forms an additional hydrogen bond with the amino group of Lys146 of the opposite p50 unit (chain A) (Fig. 2, Table 3).

As previously reported for the binding mode of active compound **1** into the dimer[19], and unlike the other binders here individuated, the coumarin moiety of the active molecule **7f** was involved in two hydrogen bonds with Cys62 (here Cys59 from crystallographic structure)[26], a very important residue for NF-κB activation in vivo. It should be point out that even if compound **7f** is localized in the

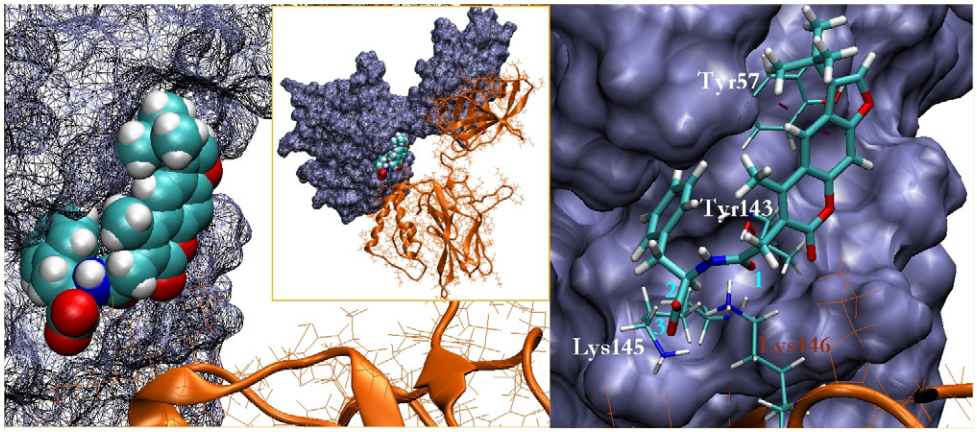

Figure 2. Stereoview of the complex formed by NF-κB p50 homodimer and the docked compound **1f**. The p50 chain B surface (purple coloured) is highlighted. Subunit p50 chain A is in NewCartoon representation with the sidechains of the residues highlighted in line drawing method. A focus of the **1f** docking pose in the DNA-binding region is shown (left and right). On the left the **1f** ligand is displayed in VDW style. On the right the key aminoacids are explicitly shown and the atoms (O.1, O.2, O.3) of compound **1f** involved in hydrogen bonds are reported. For details on protein/ligand interactions and relative distances see Table 3.

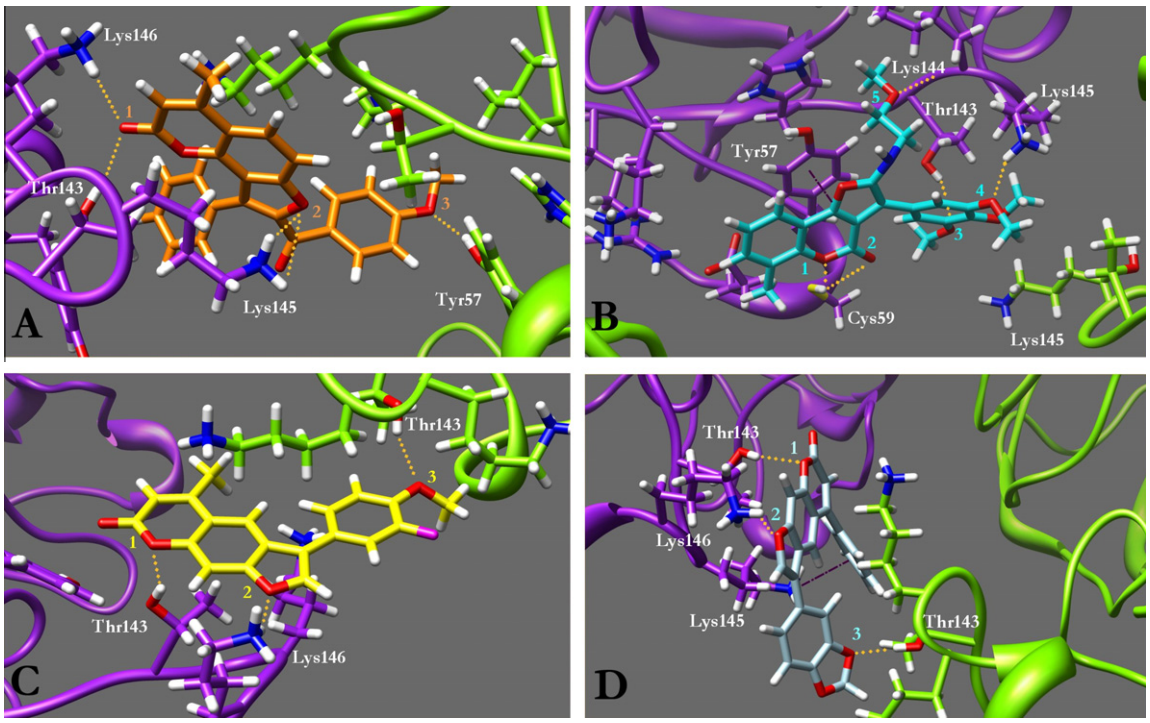

Figure 3. Close-up view of compounds **6f** (panel A, orange coloured), **7f** (panel B, cyan coloured), **9f** (panel C, yellow coloured) and **10f** (panel D, light blue coloured) binding modes into NF-κB p50 homodimer. NF-κB p50 subunits (chain A, green coloured; chain B purple coloured) are in ribbons representation. The hydrogen bonds (yellow lines), π–π interactions (violet lines) and numerations of ligand key atoms are shown. For details on protein/ligand interactions distances see Table 3.

solvent-filled cavity between the N-terminal domains of each p50 subunit, in common with the other described ligands, any over described stabilizing interaction with the second p50 subunit (chain A) has been found. Moreover, **7f** presents the same putative binding conformation into p50 monomer (GlideScore = 6.65 kcal mol^{-1}; E-Model = −43.1 kcal mol^{-1}) with a G-score value slightly lower probably due to the lack of hydrophobic interactions with the second subunit. These findings suggest that **7f** may form stable complex indifferently with both p50 monomer and dimer (Tables 2 and 3). Interestingly, compound **6f** was able to interact with the p50 monomer conformation (p50*b*) adopted into active heterodimeric state of the protein (Tables 2 and 3). Its best pose (GlideScore = −6.19 kcal mol^{-1}; E-Model = −36.8 kcal mol^{-1}) formed a hydrogen bond with Cys62 as reported for **7f** protein interaction.

The benzoquinolizin-5-one analogue **5f** does not exhibit the ability to form stable complex with NF-κB dimer, but presents the highest score into the momeric aggregation of NF-κB in comparison to the other described purchasable VS hits (Table 2). The 2-hydroxy pyridine moiety and the amide group of highest-scored pose of this ligand (GlideScore = −7.86 kcal mol^{-1}; E-Model = −46.3 kcal mol^{-1}) are involved in hydrogen bindings with Lys241, Asp239 and Tyr57, whereas its benzoquinolizin-5-one scaffold interacts with Cys62 (here Cys59 from crystallographic structure)[30], an important residue for NF-κB in vivo activity (Table 3 and Fig. 4).

Further experimental studies (based on chemical synthesis and further biological assays) for compounds **1f** and **5f** (not available commercially) will be necessary to support the NF-κB inhibitory activity suggested from our molecular modeling findings.

2.4. Biological activity of the best-scored, commercially available compounds: EMSA studies

In order to determine biological activity of the VS-selected, commercially available compounds **6f, 7f, 9f** and **10f** EMSA studies were performed.[20–23] Purified p50 NF-κB was employed for this analysis. The results obtained demonstrated that compounds **6f**, **7f**, **9f** and **10f** inhibited the formation of a stable NF-κB p50/DNA complex. The most active compounds **10f** and **9f** are psoralen derivatives and had an IC_{50} of about 20 μM (Table 4). The furo-(3,2-c)chromen-4one derivative **7f** showed an IC_{50} of about 40 μM while the angelicin derivative **6f** showed an activity of 60 μM (Fig. 5 and Table 4). These activities are quite interesting, especially after comparison with the reference furocoumarins psoralen and angelicin (Fig. 5 and Table 4),[26,27,31] with the NF-κB inhibitors pyrogallol red,[28] bromopyrogallol red,[28] 5,7-DHMC[29] and with the most active compounds found in our previously reported analysis, compound **1**[19] and compound **21**[18] (see Fig. 1 for the molecular structures and Table 4 for inhibitory activity on NF-κB/DNA interactions).

This set of experiments demonstrate that all the molecules identified by VS are, as expected, active in inhibiting the interactions between NF-κB and target DNA.

2.5. Biological activity: Inhibition of IL-8 mRNA accumulation in IB3-1-cystic fibrosis cells infected with *P. aeruginosa*

In order to determine the biological activity of compounds **6f**, **7f**, **9f** and **10f** we employed cystic fibrosis IB3-1 cells infected with P. aeruginosa. In this system NF-κB dependent genes, including those coding for the pro-inflammatory protein IL-8 are activated. This feature in very important in the pathophysiology of cystic fibrosis, since several clinical complications are caused by exacerbation of this inflammatory response.[20]

Cells were incubated overnight in the presence of compounds **6f**, **7f**, **9f** and **10f** (10 μM), then exposed to PAO1 for further 4 h. After this length of time, RNA was isolated and RT-qPCR performed to quantify the expression of IL-8 gene. The results are reported in Figure 6, which demonstrates that compounds **6f**, **7f** and **9f** inhibit PAO-1 induced IL-8 mRNA accumulation, while compound **10f** was not active. Interestingly, and well in agreement with the VS data

Table 3
Hydrogen bonds and π–π interactions of the best-ranked (**1f**) and active compounds (**6f**, **7f**, **9f**, **10f**) with the involved residues of the DNA binding region of NF-κB p50 homodimer and monomer (see Figs. 2–4 for ligands atom labels)

	Residue interaction		Ligand atom/s		Distance (Å)
DIMER	$(Cys59)_{(B)}$	–SH::O	O.1	(**7f**)	2.54
			O.2	(**7f**)	2.96
	$(Thr143)_{(B)}$	–OH::O	O.1	(**1f**)	2.06
			O.3	(**7f**)	2.52
			O.1	(**6f**)	2.97
			O.1	(**9f**)	2.01
			O.1	(**10f**)	2.20
	$(Lys145)_{(A)}$	$–N^+–H::O$	O.3	(**1f**)	2.73
	$(Lys145)_{(B)}$	$–N^+–H::O$	O.2	(**6f**)	2.85
			O.2	(**6f**)	2.02
			O.4	(**7f**)	2.14
	$(Lys145)_{(B)}$	$–N^+$	Aromatic moiety	(**10f**)	3.35
	$(Lys144)_{(B)}$	–NH::O	O.5	(**7f**)	2.09
	$(Tyr57)_{(B)}$	-Ph-centroid	Aromatic moiety	(**1f**)	3.93
		centroid-	Aromatic moiety	(**7f**)	3.57
	$(Tyr57)_{(A)}$	–OH::O	O.3	(**6f**)	1.80
	$(Lys146)_{(B)}$	$–N^+–H::O$	O.2	(**1f**)	2.57
			O.1	(**6f**)	2.9
			O.2	(**9f**)	1.85
			O.2	(**10f**)	2.0
	$(Thr143)_{(A)}$	–OH::O	O.3	(**9f**)	2.41
			O.3	(**10f**)	2.15
MONOMER	$(Tyr57)_{(p50b)}$	-Ph-centroid	Aromatic moiety	(**6f**)	3.88
		centroid-			
	$(Cys59)_{(p50b)}$	–SH::O	O.4	(**6f**)	2.45
	$(Lys146)_{(p50b)}$	$–N^+–H::O$	O.3	(**6f**)	2.41
	$(Lys241)_{(p50b)}$	$–N^+–H::O$	O.1	(**6f**)	1.93
	$(Tyr57)_{(p50b)}$	-Ph-centroid	Aromatic moiety	(**7f**)	3.87
		centroid-			
	$(Cys59)_{(p50b)}$	–SH::O	O.1	(**7f**)	2.53
			O.2	(**7f**)	2.97
	$(Lys144)_{(p50b)}$	–NH::O	O.5	(**7f**)	2.25
	$(Lys145)_{(p50b)}$	$–N^+–H::O$	O.4	(**7f**)	1.93
	$(Tyr57)_{(p50a)}$	–O::HN	H.1	(**5f**)	2.09
	$(Asp239)_{(p50a)}$	$–COO^–::HO$	H.2	(**5f**)	1.68
	$(Lys241)_{(p50a)}$	$–N^+–H::O$	O.1	(**5f**)	2.23

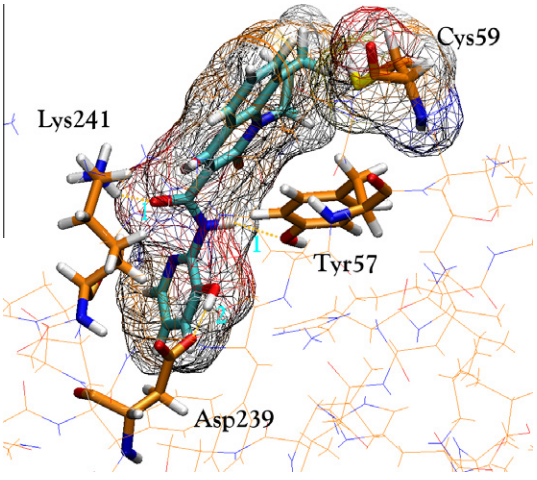

Figure 4. The highest-scored pose of compound **5f** docked into NF-κB p50 monomer. The intermolecular hydrogen bonds (yellow lines) and molecular surfaces (ligand and Cys59) are shown. The numerations of **5f** key atoms are highlighted. For details on protein/ligand interactions distances see Table 3.

shown in Table 2, compound **6f** was the most active in inhibiting PAO-1 induced IL-8 mRNA accumulation in IB3-1 cells. Further experiments are needed to understand the lack of activity of compound **10f** on IL-8 gene expression in PAO-1 infected IB3-1 cells. In addition, we like to underline that the differences between the results on the activity of the compounds determined following EMSA studies (Fig. 5) and cellular treatment (Fig. 6) are largely expected. In fact, the EMSA analysis reported in Figure 5 is based on molecular interactions between target DNA sequences and purified NF-κB p50, while within cellular systems the occurring interactions are much complex, since several proteins belonging to the NF-κB family are present together with a variety of NF-κB regulators; all these proteins, at least in theory, might be differentially affected by the compounds selected with the VS procedure here described.

These results demonstrate that treatment of CF IB3-1 cells with **6f**, **7f** and **9f** significantly reduces the PAO1-dependent transcription of the pro-inflammatory mediator IL-8.

Table 4
Inhibition of NF-κB/DNA interactions[a]

Compound	Inhibition of NF-κB/DNA interactions	References
6f	60 μM	This work
7f	40 μM	This work
9f	20 μM	This work
10f	20 μM	This work
Psoralen	3 mM	This work
Angelicin	2.5 mM	This work
Pyrogallol red	10 μM	Sharma et al.[28]
Bromopyrogallol red	30 μM	Sharma et al.[28]
5,7-DHMC	200 μM	Sharma et al.[29]
1	50 μM	Piccagli et al.[19]
21	5 mM	Piccagli et al.[18]

[a] IC_{50}, concentrations required to reach 50% inhibition of NF-κB/DNA interactions.

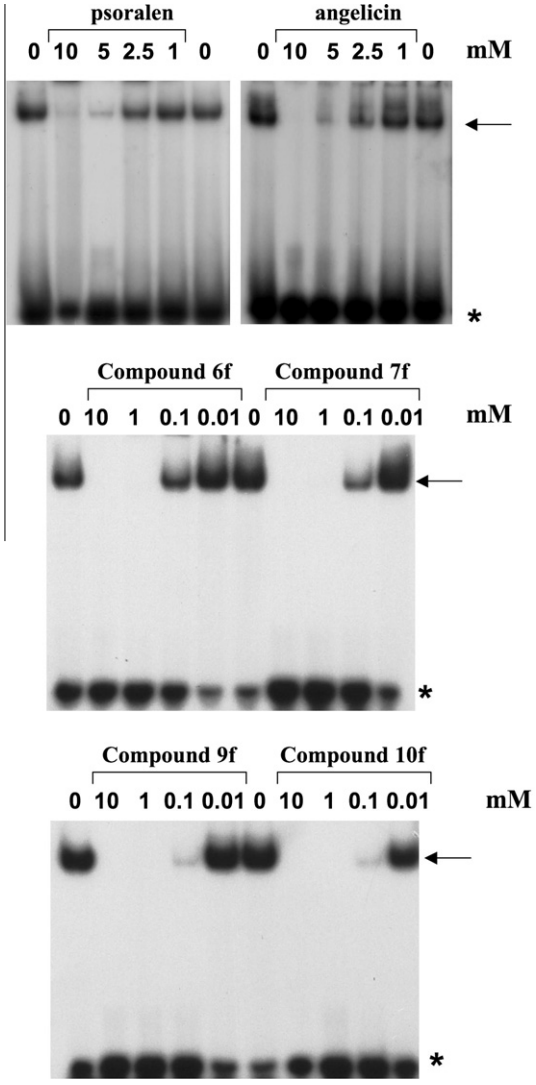

Figure 5. Effects of psoralen, angelicin, and compounds **6f**, **7f**, **9f** and **10f** on the molecular interactions between NF-κB p50 and ^{32}P-labelled target NF-κB double stranded oligonucleotide. Compounds were first incubated with NF-κB and then the ^{32}P-labelled target NF-κB oligonucleotide was added. NF-κB/DNA complexes were analyzed by polyacrylamide gel electrophoresis. Arrows indicate NF-κB/DNA complexes; asterisks indicate the ^{32}P-labelled target NF-κB probe.

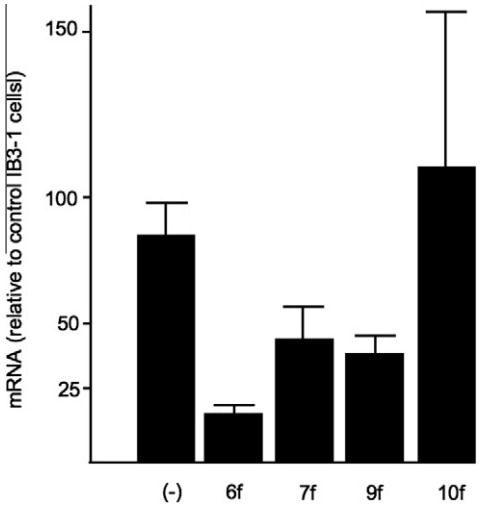

Figure 6. Effects of compounds **6f**, **7f**, **9f** and **10f** on IL-8 gene expression in *Pseudomonas aeruginosa* infected cells. IB3-1 cells were exposed for 24 h to 50 μM compounds and the infected with PAO1 as described in methods. After further 4 h RNA was isolated and quantitative RT-PCR performed. IL-8 mRNA content is quantified in respect to control uninduced IB3-1 cells.

3. Conclusions

The VS method we adopted against NF-κB p50 lead to the individuation of four interesting, commercially available, furocumarin derivatives able to inhibit the NF-κB/DNA complex formation. The reported putative protein binding modes of these substituted psoralen, angelicin and furo(3,2-c)chromen-4one structures have been individuated and described, hinting new strategy for future design of NF-κB activity modulators ligands. Moreover, other chemical molecular structures have been suggested as potentially NF-κB inhibitors from our VS studies (**1f**–**5f**). In particular, the docking results for the benzoquinolizin-5-one analogue **5f** show that 1-amide 2-hydroxy pyridine moiety may be important for NF-κB p50 interaction.

The forward filtering strategy based on the chemical motifs showed to be useful for the target under study. Our computational results in according with experimental studies, demonstrate that interesting motifs can be used to focusing prepared the initial database for a subset of compounds to be docked into NF-κB. Furthermore, we have demonstrated that docking simulations are suitable for predictive studies on binding affinity of small compounds to a difficult target as NF-κB. With these results we think to have laid the foundations for the development of further successful VS applications against NF-κB and computational lead optimizations studies.

As far biomedical applications, it should be underlined that NF-κB is involved in several human pathologies, including osteoporosis,[32] rheumatoid arthritis[33] and cancer.[34] In addition, NF-κB is one among the master transcription factors responsible of the induction of pro-inflammatory genes in cystic fibrosis cells infected with P. aeruginosa or treated with TNF-α. Our data suggest that the identified molecules might be of interest for experimental therapy of cystic fibrosis. In fact, a strong anti-inflammatory effect of compounds **6f**, **7f** and **9f** has been detected after challenging IB3-1 bronchial CF cells with TNF-α. Recent results, suggesting that compound **1f** and analogues efficiently inhibit NF-κB/DNA interactions (IC_{50} = 30 μM) and IL-8 gene expression in TNF-α treated IB3-1 cells, fully support the conclusions of the present paper (Borgatti et al., manuscript in preparation). Although epithelial cells lying the surface of the airway tract are considered good sensors of the activity of promising anti-inflammatory agents, the effect of compounds **6f**, **7f** and **9f** should be in the future extended also to the whole lung tissues of mice infected in vivo, in order to verify the possibility of multiple anti-inflammatory effects on different cells orchestrating the innate immune response in the lung.

4. Materials and methods

4.1. Structure-based virtual screening

All computational studies were performed on a two Intel Xeon 3.2 GHz processors on a Linux PC.

4.1.1. Preparation of the focus compounds library

Angelicin and psolaren derivatives as reported in literature[26,27] (Table 1) were build employing Maestro graphical interface supplied by Schrodinger. The three-dimensional geometry of each molecule was minimized with *bmin* by using OPLS-AA force field.[35] Natural and synthetic organic compounds available in a structure searchable database were retrieved using a substructure searching (2D) method. The distributors accessible on the network that we

successfully used are the followings: Sigma–Aldrich,[36] Maybridge,[37] Otava,[38] TimTec,[39] Chembridge,[40] and DrugBank.[41] The browsing hits were retrieved from the substructure match obtained drawing the chemical scaffolds reported in Table 1. All the molecules were collected in a single library and prepared using LigPrep[42] from Schrodinger in a standard procedure. To this aim, all the output files in 2D sdf format were converted in 3D maestro format by using *sdconvert*. All charged groups were neutralized and subsequently ionization treatment was done generating all possible states at pH of 7.4 (±2). Eventual counter ions in salts and water molecules were removed. Various tautomers for each structure were generated. The molecules with a molecular weight >800 were not considered. In order to remove all the possible problematic structures premin script from Schrodinger was employed using OPLS-AA force field for minimization process. Finally, we obtained a library of 1705 optimized compounds consisting in furocoumarin derivatives and analogues structures.

4.1.2. Protein targets data

In order to screen the starting library of 1710 structures into NF-κB, p50-p50 dimer (1NFK) and p50 monomer in three different conformations (chains A and B from 1NFK; chain B from 1LE9)[43] were prepared for subsequently docking runs as described elsewhere.[18] Briefly, all water molecules were removed, the hydrogen atoms were added to the proteins, and OPSL-2001 atom types and charges were assigned. After preparation, refinement was performed by running a ProteinPrep job on the structure using a standard procedure. Glide (Grid-based ligand docking with energetics) using Impact software version v30512 from Schrödinger[44] was employed for the definition of the putative binding site and for the calculation of OPLS-2001 van der Waals and electrostatics grids.[35] The grids were prepared reflecting the area of the DNA binding region of the proteins.

4.1.3. Docking of compounds library into DNA binding of NF-κB

All the compounds library were docked into putative binding site of the NF-κB targets employing Glide software.[44] The Standard-Precision (SP) method as implemented in Glide, was employed as first for p50 NF-κB. The maximum number of poses per ligand to pass to the grid-refinement calculation was set to 10.000. Only one good pose for each molecule was retained. Subsequently, all possible redundant structures were eliminated from the database using the table project implemented in Glide. Based on the G-score function, the highest-ranking 1000 docked ligands were selected and collected in a new multifile for further docking runs. After a minimization process in the OPLS_2001 force field by premin script, the picked out compounds were docked again into DNA recognition site, using the more CPU time-intensive and accurate Extra-Precision (XP) method. Finally, the first 10 molecules (including all the four chemical scaffolds of Table 2) with the highest-ranking poses (XP G-score value) against the most protein target were individuated as promising. Among them only five compounds were commercially available (**6–10f**). These molecule plus **1f** were further investigated. The molecules were docked into the protein targets applying the accurate XP method as described above but in this case the total number of docked retained poses for each compound was set to 100. The subsequent selection of the putative bioactive conformation within a cluster of poses for each ligand, were based on both G-score and E-model values.

4.2. Reagents

The best ranked, commercially available compounds were 8-(4-methoxybenzoyl)-4-methyl-9-phenyl-2*H*-furo[2,3-*h*]chromen-2-one (compound **6f**), 2-(2-methoxy-ethylamino)-6-methyl-3-(3,4,5-trimethoxy-phenyl)-furo[3,2-*c*]chromen-4-one (compound **7f**), 3-(3-fluoro-4-methoxy-phenyl)-5-methyl-7*H*-Furo [3,2-*g*]chromen-7-one (compound **9f**) and 3-benzo [1,3]dioxol-5-yl-5-phenyl-7H-Furo [3,2-g]chromen-7-one (compound **10f**). Compound **6f** was obtained from Chembridge Corporation (San Diego, CA, USA), compound **7f** from Enamine Europe Ltd (Riga, Latvia, LV), compounds **9f** and **10f** from OTAVA Ltd (Kiev, Ukraine). Purity of all these compounds was higher than 97%.

4.3. Cell cultures and bacteria

IB3-1 cells (LGC Promochem), derived from a CF patient with a ΔF508/W1282X mutant genotype and immortalised with adeno12/SV40,[45] were grown in LHC-8 basal medium (Invitrogen, Carlsbad, CA), supplemented with 5% FBS in the absence of gentamycin, at 37 °C/5% CO_2. The laboratory strain of *P. aeruginosa* PAO1 was grown in trypticase soy broth (TSB) or agar (TSA) (Difco, Detroit, MI).

4.3.1. Cell infection

This was performed as previously described.[21,45] Briefly, IB3-1 cells were seeded at density of 200,000 cells/cm^2, 24 h before infection. After adhesion, cells were starved in serum free LHC-8 for 18 h. Before the experiment, PAO1 from overnight cultures in TSA plates were grown in 20 ml TSB broth at 37 °C with shaking until there was an OD at 660 nm of about 1×10^9 CFU/ml, determined by dilution plating. Bacteria were washed twice by resuspension in PBS and then to a final dilution in cell culture medium. The doses of PAO1 were determined by plating aliquots of dilutions on TSA plates and are expressed as CFU/cell. Monolayers of cells were infected with PAO1 at 37 °C/5% CO_2 for 4 h with a dose ranging from 30 to 100 CFU/cell.

4.3.2. Cell treatment with VS-selected compounds

IB3-1 cells were incubated for 24 h with different concentrations of the compound under analysis and then infected with *P. aeruginosa*.[45]

4.3.3. Quantitation of transcripts of pro-inflammatory genes

This was carried out as described previously.[21] Briefly, total RNA was isolated using High Pure RNA isolation kit (Roche, Mannheim, Germany) following the Supplier's instructions. Reverse transcription (RT) was performed using the High Capacity cDNA Archive kit (Applied Biosystems, Foster City, CA): 1 μg of total RNA were reverse transcribed in the presence of random hexamers 1X, dNTPs 2.5X, RNAse Inhibitor 100 U, Multiscribe Reverse Transcriptase 250 U and Reverse Transcriptase buffer 1X in a total volume of 100 μl, for 10 min at 25 °C and 120 min at 37 °C. As negative control, the reaction was also performed in the absence of RNA. The resulting cDNA was quantified by relative quantitative real-time PCR (real-time qPCR). Real-time qPCR was performed with 25 μl reactions, in duplicate, using the Platinum SYBR Green qPCR Super Mix-UDG (Invitrogen, Carlsbad, CA) in a 1X final concentration. ICAM-1, IL-8, GRO-α, GRO-γ, IL-6 and the respective calibrator genes were amplified in separate tubes: primers were selected by Primer Express Software (Applied Biosystems, Foster City, CA) and are indicated in Table 1. Amplification conditions were: an initial denaturation/activation step of 95 °C for 2 min, followed by 50 repeats of 95 °C for 15 s and 60 °C for 30 s.

4.3.4. Proliferation assay

IB3-1 cells were seeded at a density of 100,000 cells in 24 wells plates in LHC-8 medium in presence of 5% FBS. After adhesion, cells were starved in serum free LHC-8, drug was added at serial dilutions (as indicate in figure) and incubated for further 24 h or 48 h. After this period cells were washed with PBS and detached with trypsin/EDTA. Cells were suspended in DMEM medium and counted with a Sysmex XE-2100 Cytometer (Dasit, Milan, Italy). Cell proliferation was determined as elsewhere described.[46–48]

4.3.5. Antibacterial assay

The antimicrobial activity of pharmaceutical compounds was determined by following the procedure for the Minimum Inhibitory Concentration (M.I.C.) of the National Committee for Clinical Laboratory Standards (NCCLS) (NCCLS, 1997) with some adjustments for concentration of drug. In brief, *P. aeruginosa* was cultured on plates of Trypticase Soy Agar (TSA) overnight at 37 °C. The colonies were harvested, suspended in sterile saline, and adjusted to a concentration of a 0.5 McFarland standard. The range of drug concentration tested (as indicates in figure) was prepared in 15 ml tubes containing 5 ml of Trypticase Soy Broth (TSB) starting from a 100-fold concentrated drug stock solution. McFarland 0.5 standard of *P. aeruginosa* (20 μl) was added to each tube, and samples were incubated at 37 °C for 24 h. M.I.C. is defined as the lowest concentration of compound at which there is no visible growth of the organism. In addition, the samples were read at 660 nm wavelength for quantitative analysis with a Beckman DU 640 spectrophotometer.

4.4. Electrophoretic Mobility Shift Assay (EMSA)

Electrophoretic Mobility Shift Assay (EMSA) was performed as previously described.[20,21] Briefly, double-stranded synthetic oligodeoxynucleotides mimicking the NF-κB binding (NF-κB, sense: 5′-AAT CGT GGA ATT TCC TCT-3′) have been employed. Oligodeoxynucleotides were labeled with γ^{32}-P-ATP using 10 Units of T4-polynucleotide-kinase (MBI Fermentas) in 500 mM Tris–HCl, pH 7.6, 100 mM $MgCl_2$, 50 mM DTT, 1 mM spermidine, 1 mM EDTA in the presence of 50 mCi γ^{32}-P-ATP) in a volume of 20 ml for 45 min at 37 °C. Reaction was brought to 150 mM NaCl and 150 ng complementary oligodeoxynucleotide was added. Reaction temperature was increased to 100 °C for 5 min and left diminishing to room temperature overnight. Binding reactions were set up as described elsewhere[20] in a total volume of 20 μl containing buffer TF plus 5% glycerol, 1 mM dithiothreitol, 10 ng of human NF-κB p50 protein (Promega) and different concentrations of compounds. After a incubation of 20 min at room temperature, 0.25 ng of ^{32}P-labeled oligonucleotides were added to the samples for further 20 min at room temperature and then they were electrophoresed at constant voltage (200 V) under low ionic strength conditions (0.25X TBE buffer: 22 mM Tris borate, 0.4 mM EDTA) on 6% polyacrylamide gels. Gels were dried and subjected to standard autoradiographic procedures.[20]

4.5. Statistics

Results are expressed as mean ± standard error of the mean (SEM). Comparisons between groups were made by using paired Student's *t* test and a one-way analysis of variance (ANOVA). Statistical significance was defined with $P < 0.05$.

Acknowledgments

R.G. is granted by Fondazione Cariparo (Cassa di Risparmio di Padova e Rovigo), CIB, by Telethon (contract GGP07257) and by COFIN-2007. This research is also supported by Associazione Veneta per la Lotta alla Talassemia (AVLT), Rovigo.

References and notes

1. Boucher, R. C. *Eur. Respir. J.* **2004**, *23*, 146.
2. Verkman, A. S.; Song, Y.; Thiagarajah, J. R. *Am. J. Physiol. Cell. Physiol.* **2003**, *284*, C2.
3. Welsh, J. M.; Ramsey, B. W.; Accurso, F. In *The Molecular and Metabolic Basis of Inherited Disease*; Scriver, C. R., Ed.; McGraw-Hill: New York, 2001.
4. Ratjen, F.; Döring, G. *Lancet* **2003**, *361*, 681.
5. Bonfield, T. L.; Panuska, J. R.; Konstan, M. W.; Hilliard, K. A.; Hilliard, J. B.; Ghnaim, H.; Berger, M. *Am. J. Respir. Crit. Care Med.* **1995**, *152*, 2111.
6. Joseph, T.; Look, D.; Ferkol, T. *Am. J. Physiol. Lung Cell. Mol. Physiol.* **2005**, *288*, L471.
7. Adamo, R.; Sokol, S.; Soong, G.; Gomez, M. I.; Prince, A. *Am. J. Respir. Cell Mol. Biol.* **2004**, *30*, 627.
8. Zhang, Z.; Louboutin, J.-P.; Weiner, D. J.; Goldberg, J. B.; Wilson, J. M. *Infect. Immun.* **2005**, *73*, 7151.
9. Bonizzi, G.; Karin, M. *Trends. Immunol.* **2004**, *25*, 280.
10. Sadikot, R. T.; Zeng, H.; Joo, M.; Everhart, M. B.; Sherrill, T. P.; Li, B.; Cheng, D. S.; Yull, F. E.; Christman, J. W.; Blackwell, T. S. *J. Immunol.* **2006**, *176*, 4923.
11. Rottner, M.; Kunzelmann, C.; Mergey, M.; Freyssinet, J. M.; Martínez, M. C. *FASEB J.* **2007**, *21*, 2939.
12. DiMango, E.; Ratner, A. J.; Bryan, R.; Tabibi, S.; Prince, A. *J. Clin. Invest.* **1998**, *101*, 2598.
13. Lampronti, I.; Khan, M. T.; Bianchi, N.; Ather, A.; Borgatti, M.; Vizziello, L.; Fabbri, E.; Gambari, R. *Med. Chem.* **2005**, *1*, 327.
14. Lampronti, I.; Khan, M. T.; Borgatti, M.; Bianchi, N.; Gambari, R. *Evid. Based Complement. Alternat. Med.* **2008**, *5*, 303.
15. Nicolis, E.; Lampronti, I.; Dechecchi, M. C.; Borgatti, M.; Tamanini, A.; Bezzerri, V.; Bianchi, N.; Mazzon, M.; Mancini, I.; Giri, M. G.; Rizzotti, P.; Gambari, R.; Cabrini, G. *Int. Immunopharmacol.* **2009**, *9*, 1411.
16. Menter, A.; Griffiths, C. E. *Lancet* **2007**, *370*, 272.
17. Kitamura, N.; Kohtani, S.; Nakagaki, R. *J. Photochem. Photobiol.* **2005**, *6*, 168.
18. Piccagli, L.; Fabbri, E.; Borgatti, M.; Bezzerri, V.; Mancini, I.; Nicolis, E.; Dechecchi, M. C.; Lampronti, I.; Cabrini, G.; Gambari, R. B. M. C. *Struct. Biol.* **2008**, *8*, 38.
19. Piccagli, L.; Fabbri, E.; Borgatti, M.; Bianchi, N.; Bezzerri, V.; Mancini, I.; Nicolis, E.; Dechecchi, M. C.; Lampronti, I.; Cabrini, G.; Gambari, R. *ChemMedChem* **2009**, *4*, 2024.
20. Borgatti, M.; Bezzerri, V.; Mancini, I.; Nicolis, E.; Dechecchi, M. C.; Lampronti, I.; Rizzotti, P.; Cabrini, G.; Gambari, R. *Biochem. Biophys. Res. Commun.* **2007**, *357*, 977. Epub 2007 Apr 20.
21. Bezzerri, V.; Borgatti, M.; Nicolis, E.; Lampronti, I.; Dechecchi, M. C.; Mancini, I.; Rizzotti, P.; Gambari, R.; Cabrini, G. *Am. J. Respir. Cell. Mol. Biol.* **2008**, *39*, 86.
22. Nicolis, E.; Lampronti, I.; Dechecchi, M. C.; Borgatti, M.; Tamanini, A.; Bianchi, N.; Bezzerri, V.; Mancini, I.; Giri, M. G.; Rizzotti, P.; Gambari, R.; Cabrini, G. *Int. Immunopharmacol.* **2008**, *8*, 1672.
23. Gambari, R. *Evid. Based Complement. Alternat. Med.* **2009**. Epub ahead of print.
24. Borgatti, M.; Breda, L.; Cortesi, R.; Nastruzzi, C.; Romanelli, A.; Saviano, M.; Bianchi, N.; Mischiati, C.; Pedone, C.; Gambari, R. *Biochem. Pharmacol.* **2002**, *64*, 609.
25. Bianchi, N.; Passadore, M.; Rutigliano, C.; Feriotto, G.; Mischiati, C.; Gambari, R. *Biochem. Pharmacol.* **1996**, *52*, 1489.
26. Viola, G.; Vedaldi, D.; Dall'Acqua, F.; Lampronti, I.; Bianchi, N.; Zuccato, C.; Borgatti, M.; Gambari, R. *J. Photochem. Photobiol. B* **2008**, *92*, 24.
27. Miolo, G.; Moro, S.; Vedaldi, D.; Caffieri, S.; Guiotto, A.; Dall'Acqua, F. *Il Farmaco* **1999**, *54*, 551.
28. Sharma, R. K.; Chopra, S.; Sharma, S. D.; Pande, V.; Ramos, M. J.; Meguro, K.; Inoue, J.; Otsuka, M. *J. Med. Chem.* **2006**, *49*, 3595.
29. Sharma, R. K.; Pande, V.; Ramos, M. J.; Rajor, H. K.; Chopra, S.; Meguro, K.; Inoue, J.; Otsuka, M. *Bioorg. Chem.* **2005**, *33*, 67.
30. Muller, C. W.; Rey, F. A.; Sodeoka, M.; Verdine, G. L.; Harrison, S. C. *Nature* **1995**, *373*, 311.
31. Lampronti, I.; Bianchi, N.; Borgatti, M.; Fibach, E.; Prus, E.; Gambari, R. *Eur. J. Haemat.* **2003**, *71*, 189.
32. Piva, R.; Penolazzi, L.; Borgatti, M.; Lampronti, I.; Lambertini, E.; Torreggiani, E.; Gambari, R. *Ann. N.Y. Acad. Sci.* **2009**, *1171*, 448.
33. Penolazzi, L.; Lampronti, I.; Borgatti, M.; Khan, M. T.; Zennaro, M.; Piva, R.; Gambari, R. *BMC Complement. Altern. Med.* **2008**, *8*, 59.
34. Luqman, S.; Pezzuto, J. M. *Phytother. Res.* **2010**, *24*, 949.
35. Jorgensen, W. L.; Maxwell, D. S.; Tirado-Rives, J. *J. Am. Chem. Soc.* **1996**, *118*, 11225.
36. Sigma–Aldrich offer many services including chemical searching in basic research. http://www.sigmaaldrich.com/.
37. Maybridge chemical collection contains both biologically active compounds and molecules suitable for chemical modifications which format allows the structural analysis of the content. http://www.maybridge.com.
38. OTAVA Ltd is an international science-based chemical company founded in 1997. In-house Stock Collection contains about 156,000 compounds, made available on the web server http://www.otavachemicals.com/.
39. TimTec offers pre-designed small compound collections and the selected databases can be searched by structure/substructure/similarity online (http://www.timtec.net).
40. ChemBridge Corporation offer screening compound libraries, target focused compounds, chemical building blocks, custom compound libraries and synthetic and medicinal chemistry support services available on the web server http://www.chembridge.com.
41. DrugBank, made available on the web server http://www.drugbank.ca/.
42. Maestro (v7.0.113), Schrodinger, LLC, NY, 2005. http://www.schrodinger.com.
43. Chen, F. E.; Huang, D. B.; Chen, Y. Q.; Ghosh, G. *Nature* **1998**, *391*, 410.
44. Halgren, T. A.; Murphy, R. B.; Friesner, R. A.; Beard, H. S.; Frye, L. L.; Pollard, W. T.; Banks, J. L. *J. Med. Chem.* **2004**, *47*, 1750.
45. Dechecchi, M. C.; Nicolis, E.; Norez, C.; Bezzerri, V.; Borgatti, M.; Mancini, I.; Rizzotti, P.; Ribeiro, C. M.; Gambari, R.; Becq, F.; Cabrini, G. *J. Cyst. Fibros.* **2008**, *7*, 555.
46. Khan, M. T.; Lampronti, I.; Martello, D.; Bianchi, N.; Jabbar, S.; Choudhuri, M. S.; Datta, B. K.; Gambari, R. *Int. J. Oncol.* **2002**, *21*, 187.
47. Lampronti, I.; Martello, D.; Bianchi, N.; Borgatti, M.; Lambertini, E.; Piva, R.; Jabbar, S.; Choudhuri, M. S.; Khan, M. T.; Gambari, R. *Phytomedicine* **2003**, *10*, 300.
48. Lambertini, E.; Piva, R.; Khan, M. T. H.; Lampronti, I.; Bianchi, N.; Borgatti, M.; Gambari, R. *Int. J. of Oncol.* **2004**, *2*, 419.